



## Research

**Cite this article:** Velázquez J, Allen RB, Coomes DA, Eichhorn MP. 2016 Asymmetric competition causes multimodal size distributions in spatially structured populations. *Proc. R. Soc. B* **283**: 20152404. <http://dx.doi.org/10.1098/rspb.2015.2404>

Received: 16 October 2015

Accepted: 30 November 2015

**Subject Areas:**

ecology, theoretical biology

**Keywords:**

bimodality, individual-based model, forests, *Fuscospora cliffortioides*, southern beech, zone-of-influence

**Author for correspondence:**

Markus P. Eichhorn

e-mail: [markus.eichhorn@nottingham.ac.uk](mailto:markus.eichhorn@nottingham.ac.uk)

Electronic supplementary material is available at <http://dx.doi.org/10.1098/rspb.2015.2404> or via <http://rspb.royalsocietypublishing.org>.

# Asymmetric competition causes multimodal size distributions in spatially structured populations

Jorge Velázquez<sup>1,2</sup>, Robert B. Allen<sup>3</sup>, David A. Coomes<sup>4</sup> and Markus P. Eichhorn<sup>5</sup>

<sup>1</sup>School of Physics and Astronomy, The University of Nottingham, Nottingham NG7 2RD, UK

<sup>2</sup>Facultad de Ciencias Físico Matemáticas, Universidad Autónoma de Puebla, Puebla, Pue. 72001, México

<sup>3</sup>Landcare Research, P.O. Box 69, Lincoln 8152, New Zealand

<sup>4</sup>Forest Ecology and Conservation Group, Department of Plant Sciences, University of Cambridge, Downing Street, Cambridge CB2 3EA, UK

<sup>5</sup>School of Life Sciences, The University of Nottingham, University Park, Nottingham NG7 2RD, UK

Plant sizes within populations often exhibit multimodal distributions, even when all individuals are the same age and have experienced identical conditions. To establish the causes of this, we created an individual-based model simulating the growth of trees in a spatially explicit framework, which was parametrized using data from a long-term study of forest stands in New Zealand. First, we demonstrate that asymmetric resource competition is a necessary condition for the formation of multimodal size distributions within cohorts. By contrast, the legacy of small-scale clustering during recruitment is transient and quickly overwhelmed by density-dependent mortality. Complex multi-layered size distributions are generated when established individuals are restricted in the spatial domain within which they can capture resources. The number of modes reveals the effective number of direct competitors, while the separation and spread of modes are influenced by distances among established individuals. Asymmetric competition within local neighbourhoods can therefore generate a range of complex size distributions within even-aged cohorts.

## 1. Introduction

Individual organisms within natural populations usually vary greatly in size. A description of the distribution of sizes is a common starting point for many demographic studies (e.g. [1–3]). This is especially the case for plants, where size distributions are often considered to convey information regarding the stage of development of a stand or the processes occurring within a population [4]. In the absence of asymmetric competition or size-related mortality, the sizes of individuals within an even-aged cohort should be approximately normally distributed around a single mode, allowing for some variation in growth rate. More commonly, a left skew is observed during early stages of cohort development; this is attributed to smaller-sized individuals receiving insufficient resources to maintain growth, ultimately increasing their likelihood of mortality [5,6]. Size-thinning thereafter reduces the degree of skewness [7–9] such that the distribution converges on a common maximum size [2]. Finally, as individuals die through disturbance or senescence, and recruitment into lower size classes occurs, populations shift to a size distribution referred to as reverse J-shaped, where a high density of small individuals is combined with a small number of large dominants. This is a common pattern in old-growth forests, especially those dominated by shade-tolerant species that can persist in small size classes (e.g. [10]).

A range of statistical models exist to capture these transitions in size distributions [4,11]. Nevertheless, such simple models are unable to capture the behaviour of many systems. Multimodality of size distributions is widely observed in nature [2,7,12]. This is particularly true of plant populations (see

**Table 1.** Model terms as used in the text, separated between fitted parameters obtained from field data and free variables at the individual and stand levels. dbh, diameter at breast height.

symbol	value	units	definition
fitted parameters			
$a$	$2.5 \times 10^{-3}$	$10 \times \text{kg}^{-3/4} \text{yr}^{-1}$	conversion factor between $m^{-3/4}$ and $E$
$b$	$2.5 \times 10^{-4}$	$10 \times \text{kg}^{-1}$	resource cost for maintenance per unit biomass
$C_{\text{dbh}}$	9.4	cm per $(10 \times \text{kg}^{3/8})$	allometric relation between biomass and dbh
individual-level parameters			
$m$	variable	$10 \times \text{kg}$	biomass of an individual
$d_j$	variable	m	distance between an individual $i$ and its neighbour $j$
$A_j^i$		$\text{m}^2$	area of interaction between an individual $i$ and its neighbour $j$
stand-level parameters			
$p$	fixed	dimensionless	degree of competitive asymmetry. $p = 0$ corresponds to symmetric competition while $p > 0$ indicates asymmetric competition
$E$	equation (2.3)	$10 \times \text{kg} \text{yr}^{-1}$	resource intake rate of an individual
$I(m, m_j, d_j)$	equation (2.4)	resource $\text{yr}^{-1}$	reduction of resource intake rate due to competition
$f_m(m, m_j)$	$m^p / (m^p + m_j^p)$	dimensionless	fraction of resources that an individual of biomass $m$ obtains from the area of interaction with an individual of biomass $m_j$

table 1 in [13]), even when all individuals are known to have recruited simultaneously [14]. The prevalence of multimodality is likely to have been underestimated due to a failure to apply appropriate statistical tests (e.g. [15]). In some studies, even when multimodal distributions are observed, they are overlooked or dismissed as anomalous (e.g. [8,11,16]).

When larger organisms monopolize access to resources this increases the asymmetry of competition among individuals [17]. Small individuals face combined competition from all neighbours larger than themselves, whereas large individuals are unaffected by their smaller neighbours. This is particularly likely to be the case for light competition among vascular plants, where taller stems capture a greater proportion of available radiation and determine access for those beneath [18]. As larger individuals can thereby maintain higher growth rates, incipient bimodality will be reinforced [12], at least until light deprivation causes mortality among smaller individuals [1]. Stand development models are able to generate bimodal patterns when resources for growth become limited [19–21]. Nevertheless, though the potential for bimodality to arise from competitive interactions is well known, previous models have only been able to reproduce it within a narrow range of parameters [19,20], leading to the conclusion that it is the least likely cause of bimodality in natural size distributions [12]. A range of alternative mechanisms might give rise to multimodality, including abiotic heterogeneity whereby large stem sizes are indicative of favourable environmental conditions [22], or sequential recruitment of overlapping cohorts [12]. Finally, the initial spatial pattern of recruits may itself create complex variation in the sizes of individuals.

In this study, we argue that instead of being unusual or aberrant, multimodality is an expected outcome whenever strong asymmetries in competition among individuals occur in cohorts of sessile species. We sought to determine the conditions under which multimodal size distributions form in spatially structured populations using an individual-based modelling approach. Such models have the potential

to derive new insights into fundamental ecological processes as they often demonstrate emergent properties that cannot be predicted from population-level approaches [23]. In order to parametrize our models, we used a long-term dataset of 250 plots in New Zealand in which the sizes of over 20 000 *Fuscospora cliffortioides* (Hook. f.) Heenan & Smissen ( $\equiv$  *Nothofagus solandri* var. *cliffortioides* (Hook. f.) Poole) trees have been monitored since 1974 [9,24,25]. These data are used to obtain plausible parameters for our simulation model, which is then employed to explore the causes of multimodality in virtual populations.

Our predictions were that (i) the size distribution of individuals would carry a long-term signal of the spatial patterns at establishment, and that (ii) asymmetries in competitive ability would increase the degree of bimodality, which once established would strengthen through time, until resource deprivation removed weaker competitors from the population. Finally, we aimed to test whether (iii) manipulating the distance and number of competitors within local neighbourhoods would generate variation in the number and positions of modes within cohort size distributions. Through this work, we demonstrate that complex size distributions with multiple modes can be generated within cohorts even in homogeneous environmental space and when individuals are initially arranged in a regular grid. We show that multimodality is not a transient phase, but is maintained for the projected lifespan of a cohort. Finally, we show that the eventual size reached by any individual depends upon interactions with others in its immediate neighbourhood throughout its lifetime.

## 2. Material and methods

### (a) The simulation model

All parameters used in the text are summarized in table 1. The growth model is derived from a basic energy conservation principle. We assume throughout that resources in the model refer to

light (and therefore carbohydrates acquired through photosynthesis), though in principle the model could be extended to other resources with appropriate parametrization. Recruitment and age-related senescence are not included in the model. The resources  $E$  that an individual acquires in a unit of time  $t$  are distributed between the resources used to increase its size  $M_g$  and all other metabolic and maintenance costs  $M_m$ . This is expressed mathematically as a general energy budget  $E = M_g + M_m$ . Assuming that resource intake scales with biomass  $m$  as  $E \propto m^{3/4}$  [26], and a linear relation between maintenance costs and biomass  $M_m \propto m$ , we can write a simple individual growth rate equation:

$$\frac{dm}{dt} = am^{3/4} - bm, \quad (2.1)$$

where  $a$  and  $b$  are constants and the units are chosen such that an increase of one unit in biomass requires one unit of resources. A mathematically equivalent model, but with slightly different interpretation, has been proposed previously [18,27,28]. Equation (2.1) describes the potential growth rate of an individual in the absence of competition.

The potential rate of energy uptake of an individual is reduced when it competes with neighbours and thus they share the available light. In order to take this into account the growth rate in the presence of competition can be expressed as:

$$\frac{dm}{dt} = am^{3/4} - bm - \sum_j I(m, m_j, d_j), \quad (2.2)$$

where  $I_j$  represents the reduction in biomass growth of a given individual due to competition with another individual  $j$  of mass  $m_j$  and at a distance  $d_j$  from the focal tree. The competitive response is obtained by summing  $I_j$  over all interacting neighbours. We only took pairwise interactions into account, summed across all interactions for each individual. This maintained computational efficiency of the simulations [29]. An individual died if its maintenance needs  $M_m$  were not met, i.e. if  $am^{3/4} - \sum_j I(m, m_j, d_j) < bm$ .

Spatially explicit interactions among individuals were modelled with a circular zone of influence (ZOI), where  $A$  represents the potential two-dimensional space within which a plant acquires resources in the absence of competition. Resource competition between an individual  $i$  and its neighbour  $j$  is defined as occurring when  $A_i$  overlaps with  $A_j$ . Within the area of overlap,  $A^{(l)}$ , resources are distributed among the two individuals, but not necessarily equally. A larger individual (greater  $m$ ) will be a stronger competitor, for example, by over-topping in light competition, but also potentially through directing greater investment into below-ground resource capture (e.g. [30]). To incorporate asymmetric competition, we define  $f_m(m, m_j)$  as being the proportion of resources  $E$  that an individual of size  $m$  obtains from the area within which it interacts with another individual of size  $m_j$ . Assuming homogeneous resource intake within  $A$ , then  $E$  is proportional to  $A^{(o)} + f_m(m, m_j)A^{(l)}$ , where  $A^{(o)}$  is the area within which no interaction occurs ( $A - A^{(l)}$ ).

As in the absence of competition  $E = am^{3/4}$ , competition will reduce  $E$  as follows:

$$E = am^{3/4} - (1 - f_m(m, m_j))A^{(l)} \quad (2.3)$$

and

$$I(m, m_j, d_j) = (1 - f_m(m_j))A_j^{(l)}. \quad (2.4)$$

The explicit functional form for asymmetric competition is  $f_m(m, m_j) = m^p / (m^p + m_j^p)$ . When  $p = 0$ , the resources in the zone of overlap are divided equally, irrespective of each individual's size. If  $p = 1$ , then each individual receives resources in proportion to its size, and if  $p > 1$ , then larger individuals gain a disproportionate benefit given their size. This differs from a previous formulation [31], though their terminology of competitive

interactions can be matched to this work as absolute symmetry ( $p = 0$ ), relative symmetry ( $p = 1$ ) and true asymmetry ( $p > 1$ ). The shape of the competition kernel is identical in all cases.

This mathematical framework was used to create a spatially explicit simulation model in which the growth and interactions among large numbers of individuals could be assessed simultaneously.

## (b) Model fitting

To obtain realistic parameters for the simulation model, we used data from monospecific *F. cliffortioides* forests on the eastern slopes of the Southern Alps, New Zealand. *F. cliffortioides* is a light-demanding species that recruits as cohorts in large canopy gaps, and has a lifespan that seldom exceeds 200 years. The data consisted of records from 20 330 trees situated in 250 permanently marked plots that randomly sample 9000 ha of forests. Each plot was 20 × 20 m in size. In the austral summer of 1974–1975 all stems greater than 3 cm diameter at breast height (dbh) were tagged and dbh recorded. The plots were recensused during the austral summers of 1983–1984 and 1993–1994. Only stems present in more than one census were included. Previous work on this system has confirmed a dominant role for light competition in forest dynamics [9,18].

We tested the tree-size distribution from the first survey of each plot for multimodality by fitting a finite mixture model of one, two and three normal distributions (see table 1). We employed an expectation-maximization algorithm [32] within the R package `FLEXMIX` 2.3–4 [33] and used the Bayesian information criterion to decide whether each size distribution was unimodally or multimodally distributed.

In order to fit the simulation model to the data, we estimated the mass  $m$  of the trees by the allometric relation  $\text{dbh} = C_{\text{dbh}}m^{3/8}$  [26,34], where  $C_{\text{dbh}}$  was taken as a free parameter. The area  $A$  of the circle representing the potential space for resource acquisition was given by  $cA = am^{3/4}$ , where  $c$  is a proportionality constant. A linear relation between dbh and radius of the ZOI was chosen, and a high degree of asymmetric competition ( $p = 10$ ). The latter improved overall fit of the models, indicating a role for asymmetric competition in driving stand dynamics.

For each of 250 plots, we began the simulation model with the observed stem sizes from 1974 attached to points randomly distributed in space. The simulation was run for 19 model years, developed in time increments  $\delta t$  that nominally correspond to 10 weeks (for simplicity there is no seasonality of growth). An individual's growth is given by

$$\delta m_i = \left[ am_i^{3/4} - bm_i - \sum_j \frac{m_j^p}{m_i^p + m_j^p} cA_j^{(l)} \right] \delta t. \quad (2.5)$$

In each Monte Carlo iteration individuals  $m_i$  were selected at random and their size updated. A search algorithm was employed to find values of  $a$  and  $b$  that gave the best fit to the observed individual growth rates with Pearson's  $\chi^2$ , averaged across the ensemble of simulations. Note that the model was fit to the growth rates of individual stems based on repeated measurements, rather than stand-level properties such as size distributions.

Having obtained suitable values for  $a$  and  $b$ , we performed simulations to compare the size distributions as predicted by the model (assuming initially random stem positions) with the empirical distributions observed in the dataset. These were initiated using size distributions from stands in the *F. cliffortioides* dataset in which the mean stem diameter was small ( $\bar{d} < 15$  cm), then run until the mean reached a medium ( $15 \text{ cm} \leq \bar{d} < 22$  cm) or large ( $\bar{d} \geq 22$  cm) stem size. Estimates of size-dependent mortality rate were also obtained and compared with empirical outputs as in Coomes & Allen [9]. This provides an independent

evaluation of model performance as mortality rates were not used to parametrize the model.

### (c) Exploring multimodality in size structure

The simulator with fitted parameters as described above was used to explore the factors that cause multimodal size distributions to form. We tracked the development of size structures in simulated stands with differing initial spatial patterns and symmetry of competition. In these simulations, all individuals were of identical initial size.

First 2100 spatial patterns were generated, each containing a distribution of points with  $x$ - and  $y$ -coordinates in a virtual plot of  $20 \times 20$  m. Equal numbers patterns were clustered, random and dispersed. Random patterns were produced using a uniform Poisson process with intensity  $\lambda = 0.05$  points  $\text{m}^{-2}$ . Clustered patterns were created using the Thomas process. This generated a uniform Poisson point process of cluster centres with intensity  $\lambda = 0.005$ . Each parent point was then replaced by a random cluster of points, the number of points per cluster being Poisson-distributed with a mean of 10, and their positions as isotropic Gaussian displacements within  $\sigma = 1$  from the cluster centre. Dispersed patterns were produced using the Matern Model II inhibition process. First, a uniform Poisson point process of initial points was generated with intensity  $\lambda = 0.06$ . Each initial point was randomly assigned a number uniformly distributed in  $[0, 1]$ , representing an arrival time. The pattern was then thinned by deletion of any point that lay within a radius of 1.5 units of another point with an earlier arrival time. All patterns were generated in R using the `spatstat` package [35]. Each pattern contained roughly 500 points (clustered  $N = 501 \pm 2.7$ , random  $N = 501 \pm 0.8$ , dispersed  $N = 488 \pm 0.7$ ). The slightly lower number of points in the dispersed pattern reflects the inherent difficulties in generating a dense pattern with a highly dispersed structure and has no qualitative effect on later analyses. Although the density within starting patterns was approximately a quarter of that observed in the empirical data, initial density has a limited effect on final outcomes as its main effect is to reduce the time until points begin to interact [36], and lower point densities increased computational speed, allowing for greater replication.

A number of further patterns were generated to explore the influence of specific parameters. First, a regular square grid was used with a fixed distance of 1.5 or 3 m between individuals. Next, groups of individuals were created in which all individuals within groups were 3 m apart, but with sufficient distance among groups that no cross-group interactions could take place. Groups contained either two individuals (pairs), three individuals in a triangular arrangement (triads) or four individuals in a square arrangement (tetrads). The total starting population in each pattern was approximately 7500 individuals.

We ran simulations of the spatially explicit individual-based model, varying the degree of asymmetric competition  $p$ . The points generated above became individual trees represented as circles growing in two-dimensional space. Each individual was characterised by its mass  $m$  and coordinates. In order to model mortality, an individual was removed from the simulation if carbon losses exceeded gains, that is if  $[am_i^{3/4} - bm_i - \sum_j m_j^p / (m_i^p + m_j^p) A_j^{(l)}] < 0$ .

The predicted size distribution and mortality rate of clumped, random and dispersed starting patterns were obtained from ensemble averages of 700 simulations corresponding to the point processes generated above.  $m$  was a continuous variable but in order to derive the size distribution, growth and death rates, we calculated size frequencies based on 10 kg biomass bins. As the death rate changes through time due to alterations in the size structure of the community, we present the average death rate for each size class across all time steps in simulations, which run for 460 model years (at which point only a few very large stems remain).

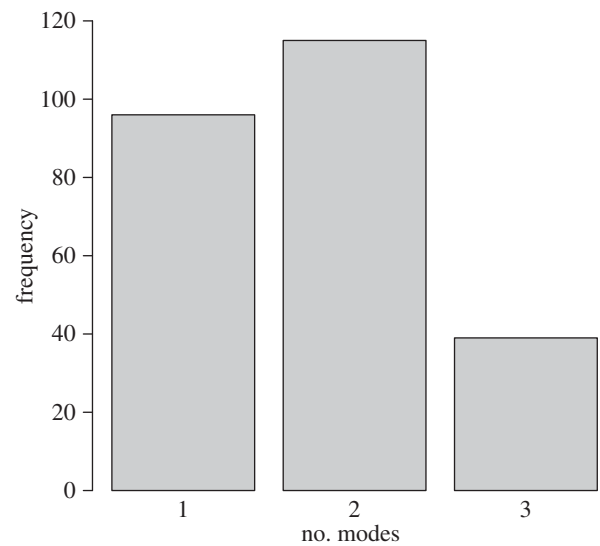


**Figure 1.** Frequency of *Fuscospora cliffortioides* plots in New Zealand exhibiting uni- or multimodality in size distribution as determined by finite mixture models testing for the presence of one, two or three modes. Data from initial 1974 to 1975 surveys.

This allows sufficient resolution for figures to be presented as effectively continuous responses rather than histograms, and is equivalent to a landscape-scale aggregation of size-dependent mortality data across a series of stands of differing ages.

## 3. Results

Analysis of the New Zealand forest plot dataset revealed multimodal distributions in 179 plots in 1974, 163 plots in 1984 and 152 plots in 1993 from of a total of 250 plots in each survey. This represents 66% of plots, showing that multimodality is more common than unimodality within these forests (see figure 1).

The simulation model was fit to the observed individual growth rates in the *F. cliffortioides* dataset and provided a robust representation of the empirically measured patterns. The fitted parameters ( $a$ ,  $b$  and  $C_{\text{dbh}}$ ) are shown in table 1. The effectiveness of the model was assessed through its ability to capture size-dependent mortality rates, which were an emergent property of the system and not part of the fitting process. Size distributions thus obtained were qualitatively similar to those observed in the empirical dataset [9] (see electronic supplementary material S1).

Subsequent simulation modelling used the parameters derived from the *F. cliffortioides* dataset ( $a$ ,  $b$ ,  $C_{\text{dbh}}$ ) and created simulated forests to investigate the potential origins of multimodal patterns. Using stochastically generated starting patterns, major differences were evident in the patterns of growth and survival depending on the degree of competitive asymmetry  $p$  and the initial spatial configuration (figure 2).

With completely symmetric competition among individuals ( $p = 0$ ), average tree growth in clustered patterns was greater than in either random or dispersed patterns (figure 2a). This unexpected result can be attributed to the high rate of density-dependent mortality in very early time steps (figure 2d). Initial mortality in random patterns reduced the population to be comparable with dispersed patterns, compensating for the slight initial differences in abundance. Clustered populations remained larger in average stem size

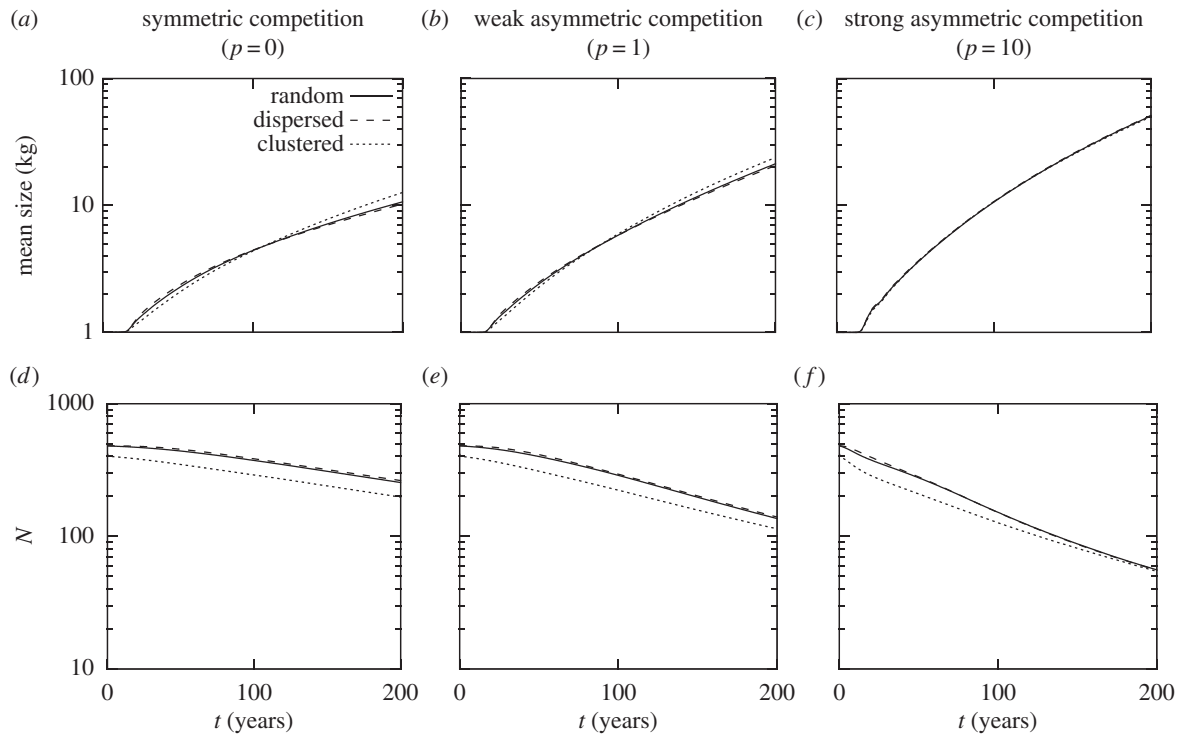


**Figure 2.** Cohort-level characteristics of stands with either random, clustered or dispersed initial starting patterns over  $t$  years (simulation time). (a–c) Mean tree size in kilograms with competition varying from (a) symmetric ( $p = 0$ ) to (b) weakly asymmetric ( $p = 1$ ) and (c) strongly asymmetric ( $p = 10$ ); (d–f) mean number of surviving individuals  $N$  per  $20 \times 20$  m plot with increasing levels of asymmetric competition  $p$  (0, 1, 10). Each line is derived from an ensemble average of 700 simulations.

(figure 2a) as the result of a smaller final population size (figure 2d), an effect that developed rapidly and was maintained beyond the plausible 200-year lifespan of *F. cliffortioides*.

In the absence of asymmetric competition ( $p = 0$ ), starting patterns had a limited effect on final size distributions, with only minor increases in skewness in clustered populations at advanced stages of development (electronic supplementary material S2). In all cases, size distributions remained unimodal. It is therefore apparent that variation in initial spatial patterns is not in itself sufficient to generate multimodality in size distributions, at least not unless the average distance among individuals exceeds their range of interaction, which is highly unlikely in the context of plant populations.

The introduction of weak asymmetry ( $p = 1$ ) tended to increase the mean size of individuals while causing reductions in population size (figure 2b,e) and diminishing the differences among initial patterns, such that with strong asymmetry ( $p = 10$ ) the differences in final size were negligible (figure 2c). Strong asymmetry also caused population sizes to converge within the likely lifespan of the trees, irrespective of starting conditions, and at a lower final level (figure 2f). Reduced differences among initial patterns with increasing asymmetry arose because fewer small trees survived around the largest tree in the vicinity, which caused patterns to converge on a state with dispersed large individuals and smaller individuals in the interstices. More left-skewed distributions also emerged as a consequence of the low tolerance of individuals to depletion of resources (individuals failing to obtain sufficient resources for their metabolic needs died immediately). Thus the small individuals die soon after their resource acquisition area is covered by the interaction range of a larger individual. Such left skew would be reduced for species capable of surviving long periods of time with low resources either through tolerance or energy reserves.

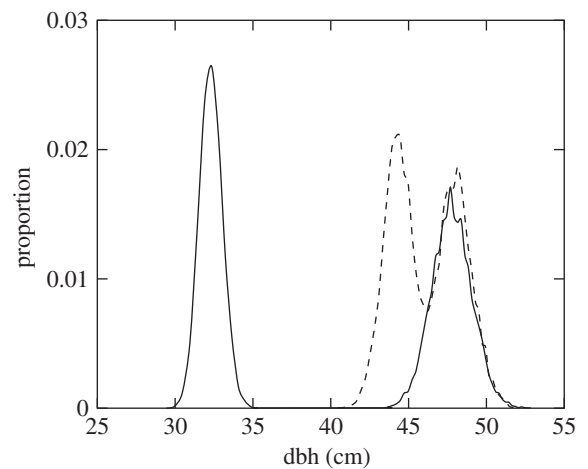


**Figure 3.** Separation between modes with varying distance of competing neighbours and strong asymmetric competition ( $p = 10$ ). Size distributions of stands composed by pairs of equidistant individuals after 200 years of development. Solid line: individuals spaced at 1.5 m, dashed line: individuals spaced at 3 m. Each line is derived from an ensemble average of 700 simulations.

Increasing competitive asymmetries caused size distributions to exhibit slight multimodality, with a lower frequency of individuals in the smaller size class at 150 years (electronic supplementary material S3). Given entirely random starting patterns, more pronounced bimodality emerged as the degree of asymmetric competition increased. Furthermore, the model predicted a U-shaped size-dependent mortality rate, qualitatively consistent with a pattern in the empirical data (see electronic supplementary material S4; cf. fig. 5 in [9]). This trend intensified with increasing asymmetric competition, and was absent when resource division was symmetric. It occurred because in large trees the

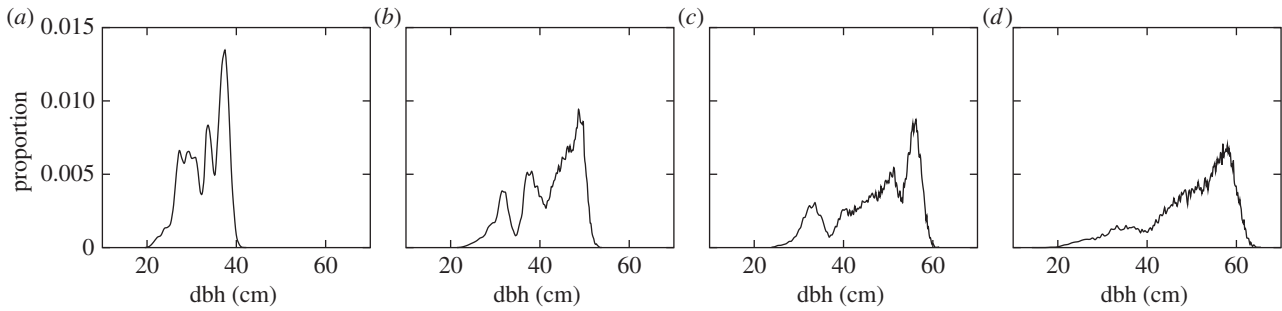


**Figure 4.** Emergent size distribution through stand development given an initially gridded starting pattern. Individuals separated by 1.5 m from their neighbours and with strong asymmetric competition ( $p = 10$ ). (a–d) distribution at 150, 200, 230 and 250 years. Each plot is derived from an ensemble average of 700 simulations.

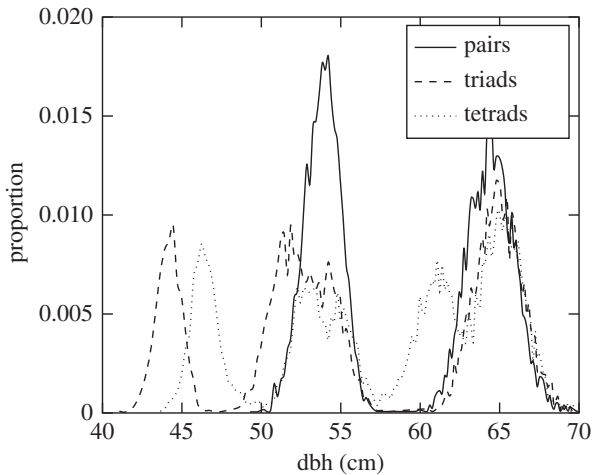


**Figure 5.** Size distributions of stands composed of groups of two, three and four equidistant competing individuals (pairs, triads and tetrads, respectively) with 3 m of separation among individuals in each group. Asymmetric competition set at  $p = 10$ . Each line is derived from an ensemble average of 700 simulations and shows the distribution at 250 years.

majority of resources are required for maintenance, and therefore even a relatively small amount of competition ultimately increases their mortality rate. In the absence of asymmetric competition the death rate of large trees approached zero.

Greater insights into the causes of multimodality are revealed through the use of designed spatial patterns in which the timing of interactions within model development can be precisely controlled. These illustrate that the separation between modes is determined by the distance among competing individuals under asymmetric competition (figure 3 and electronic supplementary material S5). The size structure can therefore provide an indication of the dominant distance over which individuals are competing, though separation of modes will be less clear when a strict grid is absent. Note that the position of the right-hand mode remains identical, and it is only the mode of the subordinate individuals that shifts to a smaller size class.

Highly dispersed patterns give rise to more complex size distributions through their development when asymmetric competition is present. In the most extreme case, when initial patterns are gridded, each individual interacts with a series of neighbours as its size increases, leading to a complex

multimodal pattern, at least until continued mortality removes smaller size classes (figure 4). Note that the modes are more clearly distinguished than is the case for random starting patterns where distances among individuals vary (cf. electronic supplementary material S3(c)).

The patterns generated by small groups of interacting individuals at equal distances apart with asymmetric competition lead to size distributions with number of modes equal to the number of individuals within each group. For patterns derived from pairs of individuals, the size distribution is bimodal, and in similar fashion triads and tetrads produce size distributions with three and four modes, respectively (figure 5). Each mode corresponds to the discrete ranking of individuals within groups. This indicates that in gridded populations, as might be observed in plantations or designed experiments, the number of modes is determined by the effective number of competitors.

## 4. Discussion

Multimodality in cohort size distributions is the outcome, rather than the cause, of asymmetric competition among individuals of varying size. Regardless of initial small-scale starting patterns, size distributions remain unimodal in the case of symmetric competition among individuals. Only when larger individuals are able to acquire a greater proportion of resources from shared space does bimodality begin to emerge. Spatial patterns of established individuals can modulate these interactions, with complex multimodal distributions generated when individuals are either regularly or highly dispersed in space. The number of modes corresponds to the number of effective competitors and their separation is a consequence of average distances among individuals. Note that our simulations do not incorporate continuous recruitment; this is a reasonable assumption for systems such as *F. cliffortioides* forests, where large-scale disturbances are followed by stand replacement.

Asymmetric competition will lead to multimodal distributions at some point during stand development. We extend upon previous studies (e.g. [37]) by providing a general framework for predicting and interpreting complex size distributions in spatially structured and even-aged populations. Under light competition the modes will correspond to discrete and well-defined canopy layers. In [13], a series of controlled experiments were conducted to investigate size distributions in populations of annual plants, finding in many cases that

distributions with two or three modes were observed. Our results allow for a fuller interpretation of these earlier findings, as we have shown that the number of modes reflects the number of effective competitors, placing a limit on the complexity of size distributions. As demonstrated in figures 3 and 5, the larger mode remains in the same position regardless of the size at which competition begins. This highlights that those individuals in larger size classes are almost unaffected by competition during stand development.

Even when all individuals in a cohort begin with identical size, small fluctuations in the acquisition of shared resources lead to a multimodal size distribution, regardless of whether the initial pattern was random, dispersed or clustered. The size distribution is not affected by differences in the initial spatial structure at small scales due to the death of close neighbours early in stand development. A similar result was found by Weiner *et al.* [36], who argue that the importance of recruitment patterns in generating asymmetries in competition may have been overstated. Likewise, initial density will have a limited effect on final size distributions as its main influence is on the time at which individuals begin to interact [36]. Therefore, while local interactions undoubtedly do cause competitive asymmetries (e.g. [17]), these are more relevant in determining the pattern of mortality during self-thinning rather than final size distributions, so long as the distances over which competition influences growth are larger than the characteristic scales at which initial spatial structuring occurs. In dense aggregations of recruiting plants, this is likely to be the case.

The model implies only a single resource for which individuals compete. It is typically assumed that above-ground competition for light is asymmetric, whereas below-ground resources are competed for symmetrically [38], though the latter assumption may not always be true (e.g. [39,40]). More complex zone-of-influence models can take into account multiple resources and adaptive allometric changes on the part of plants in response to resource conditions (e.g. [41,42]). Indeed, plasticity can diminish the impact of asymmetric competition [41,43]. Although below-ground interactions are challenging to measure directly, there is evidence that above- and below-ground biomass scale isometrically [44], which justifies the use of above-ground biomass to infer potential root competition. Previous work using the same data has identified a dominant role for light competition among smaller stems, with nutrient competition important at all stem sizes [18].

Forest mensuration tends to overlook the shape of size distributions in favour of summary statistics (e.g. mean size, coefficient of variation, maximum size; [45]) and may therefore miss out on valuable contextual information. While the utility of size distributions as a predictive tool for modelling dynamics has been frequently overstated [46], they can nonetheless remain a valuable indicator of past dynamics. One outcome of bimodality arising from asymmetric competition is that large and small individuals have differing spatial patterns, with the larger dispersed in space and the smaller confined to the interstices generated by the dominant competitors [47]. This can be used as a diagnostic tool as it allows this mechanism to be distinguished from abiotic heterogeneity, leading to clustering of similar sizes, or independent sequential recruitment, leading to a lack of co-associations between size classes [12]. Likewise in mixed-species stands succession can cause a multimodal pattern to emerge through aggregation of several unimodal cohorts, persisting

throughout stand development [10]. The interplay between size distributions, plant traits and disturbance can generate complex emergent patterns in forest dynamics at the landscape scale [48]. Bimodality generated by size competition among individuals is a distinct phenomenon from the bimodality in inherited size across species that is often observed in mixed-species communities (e.g. [49]). Where size histograms combine individuals from multiple species, the causes of bimodality are likely to include long-term evolutionary dynamics in addition to direct competition among individuals. Contextual information on spatial patterns, disturbance regimes and community composition are therefore essential to interpreting size distributions in natural systems.

Our models are based upon parameters obtained from a long-term dataset and can therefore be immediately transferred to a predictive framework. While the exact terms are most suited to the *F. cliffortioides* forests that form the basis of this work, it is likely that they will be applicable to any monospecific plant population. Bimodal size distributions might be overlooked where aggregate curves are drawn as composites of a large number of plots, which will tend to average out differences, or where appropriate statistical tests are not employed. We find that 66% of plot size distributions in our data are bimodal (figure 1). It is likely that these do not all represent single cohorts; for example, a severe storm in 1972 opened the canopy in some plots and allowed a recruitment pulse [24,50]. Irrespective of this, our growth model is able to capture subsequent stand development regardless of the origin of the bimodality (see electronic supplementary material S1). Our results also show that multimodality can act as an indicator of asymmetric competition. Thomas & Weiner [31] present evidence that the degree of asymmetry in natural plant populations is strong, with larger individuals receiving a disproportionate share of the resources for which they compete ( $p \gg 1$ ). The phenomenon of multimodality should therefore be widespread.

In conclusion, and in contrast with a previous review of bimodality in cohort size distributions [12], we contend that asymmetric competition is the leading candidate for explaining multimodal size distributions, and is its cause rather than the outcome. Previous simulation results suggesting that the parameter space within which multimodality occurs is limited were based on stand-level models. Through the use of individual-based models it can be demonstrated that multimodality is an expected outcome for any system in which larger individuals are able to control access to resources, and where individuals compete in space. The strength of these asymmetries determines the degree to which multimodality is exhibited, while the number and separation of modes are determined by the number of effectively competing individuals and the distances among them. While multimodality may be a transient phase within the development of our models, many forest stands exhibit non-equilibrium conditions, and indeed most natural plant populations are prevented by intermittent disturbance from advancing beyond this stage [24,50]. Consistently unimodal size distributions should be seen as the exception rather than the rule.

**Data accessibility.** Data were obtained from New Zealand's National Vegetation Survey Databank and can be accessed at <http://datastore.landcareresearch.co.nz/dataset/multimodal-size-distributions-in-spatially-structured-populations>. All C code used to run the simulations can be obtained from <https://github.com/jorgevc/IMB-SizeDependent>.

**Authors' contributions.** M.P.E. and J.V. conceived and designed the study; R.B.A. and D.A.C. provided data; J.V. carried out the statistical analyses under guidance from M.P.E., D.A.C. and R.B.A.; J.V. and M.P.E. prepared the first draft of the manuscript. All authors contributed towards manuscript revisions and gave final approval for publication.

**Competing interests.** We have no competing interests.

**Funding.** J.V. was supported by a Consejo Nacional de Ciencia y Tecnología post-doctoral fellowship (<http://www.conacyt.mx>) and by Engineering and Physical Sciences Research Council grant no. EP/K50354X/1 (<http://www.epsrc.ac.uk>) awarded to Juan Garrahan

and M.P.E. Funding for data collection was in part provided by the former New Zealand Forest Service and the New Zealand Ministry of Business, Innovation and Employment. The funders had no role in study design, data collection and analysis, decision to publish or preparation of the manuscript.

**Acknowledgements.** Raw data were obtained from plots established by John Wardle, and numerous others have been involved in the collection and management of data, particularly Larry Burrows, Kevin Platt, Susan Wisser and Hazel Broadbent. Juan Garrahan provided support and resources for the research.

## References

- White J, Harper JL. 1970 Correlated changes in plant size and number in plant populations. *J. Ecol.* **58**, 467–485. (doi:10.2307/2258284)
- Ford ED. 1975 Competition and stand structure in some even-aged plant monocultures. *J. Ecol.* **63**, 311–333. (doi:10.2307/2258857)
- Hara T. 1988 Dynamics of size structure in plant populations. *Trends Ecol. Evol.* **3**, 129–133. (doi:10.1016/0169-5347(88)90175-9)
- Newton AC. 2007 *Forest ecology and conservation: a handbook of techniques*. Oxford, UK: Oxford University Press.
- Weiner J. 1990 Asymmetric competition in plant populations. *Trends Ecol. Evol.* **5**, 360–364. (doi:10.1016/0169-5347(90)90095-U)
- Adler FR. 1996 A model of self-thinning through local competition. *Proc. Natl Acad. Sci. USA* **93**, 9980–9984. (doi:10.1073/pnas.93.18.9980)
- Mohler CL, Marks PL, Sprugel DG. 1978 Stand structure and allometry of trees during self-thinning of pure stands. *J. Ecol.* **78**, 599–614. (doi:10.2307/2259153)
- Knox RG, Peet RK, Christensen N. 1989 Population dynamics in loblolly pine stands: changes in skewness and size inequality. *Ecology* **70**, 1153–1166. (doi:10.2307/1941383)
- Coomes DA, Allen RB. 2007 Mortality and tree-size distributions in natural mixed-age forests. *J. Ecol.* **95**, 27–40. (doi:10.1111/j.1365-2745.2006.01179.x)
- Zenner EK. 2005 Development of tree size distributions in Douglas-fir forests under differing disturbance regimes. *Ecol. Appl.* **15**, 701–714. (doi:10.1890/04-0150)
- Wang X, Hao Z, Zhang J, Lian J, Li B, Ye J, Yao X. 2009 Tree size distributions in an old-growth temperate forest. *Oikos* **118**, 25–36. (doi:10.1111/j.0030-1299.2008.16598.x)
- Huston MA, DeAngelis DL. 1987 Size bimodality in monospecific populations: a critical review of potential mechanisms. *Am. Nat.* **129**, 678–707. (doi:10.1086/284666)
- Turley MC, Ford ED. 2011 Detecting bimodality in plant size distributions and its significance for stand development and competition. *Oecologia* **167**, 991–1003. (doi:10.1007/s00442-011-2048-3)
- Fricker JM, Wang JR, Chen HYH, Duinker PN. 2013 Stand age structural dynamics of conifer, mixedwood, and hardwood stands in the boreal forest of central Canada. *Open J. Ecol.* **3**, 215–223. (doi:10.4236/oje.2013.33025)
- Tanentzap AJ, Lee WG, Coomes DA, Mason NWH. 2014 Masting, mixtures and modes: are two models better than one? *Oikos* **123**, 1144–1152.
- Muller-Landau HC *et al.* 2006 Comparing tropical forest tree size distributions with the predictions of metabolic ecology and equilibrium models. *Ecol. Lett.* **9**, 589–602. (doi:10.1111/j.1461-0248.2006.00915.x)
- Bauer S, Wyszomirski T, Berger U, Hildenbrandt H, Grimm V. 2004 Asymmetric competition as a natural outcome of neighbourhood interactions among plants: results from the field-of-neighbourhood modelling approach. *Plant Ecol.* **170**, 135–145. (doi:10.1023/B:VEGE.0000019041.42440.ea)
- Coomes DA, Allen RB. 2007 Effects of size, competition and altitude on tree growth. *J. Ecol.* **95**, 1084–1097. (doi:10.1111/j.1365-2745.2007.01280.x)
- Gates DJ. 1978 Bimodality in even-aged plant monocultures. *J. Theor. Biol.* **71**, 525–540. (doi:10.1016/0022-5193(78)90323-5)
- Aikman DP, Watkinson AR. 1980 A model for growth and self-thinning in even-aged monocultures of plants. *Ann. Bot.* **45**, 419–427.
- Franc A. 2001 Bimodality for plant sizes and spatial pattern in cohorts: the role of competition and site conditions. *Theor. Popul. Biol.* **60**, 117–132. (doi:10.1006/tpbi.2001.1530)
- Getzin S, Wiegand T, Wiegand K, He F. 2008 Heterogeneity influences spatial patterns and demographics in forest stands. *J. Ecol.* **96**, 807–820. (doi:10.1111/j.1365-2745.2008.01377.x)
- Grimm V, Railsback SF. 2005 *Individual-based modeling and ecology*. Princeton, NJ: Princeton University Press.
- Allen RB, Bellingham PJ, Wisser SK. 1999 Immediate damage by an earthquake to a temperate montane forest. *Ecology* **80**, 708–714. (doi:10.1890/0012-9658(1999)080[0708:IDBAET]2.0.CO;2)
- Hurst JM, Allen RB, Coomes DA, Duncan RP. 2011 Size-specific tree mortality varies with neighbourhood crowding and disturbance in a montane *Nothofagus* forest. *PLoS ONE* **6**, e26670. (doi:10.1371/journal.pone.0026670)
- West GB, Brown JH, Enquist BJ. 1997 A general model for the origin of allometric scaling laws in biology. *Science* **276**, 122–126. (doi:10.1126/science.276.5309.122)
- West GB, Brown JH, Enquist BJ. 2001 A general model for ontogenetic growth. *Nature* **413**, 628–631. (doi:10.1038/35098076)
- Lin Y, Berger U, Grimm V, Ji Q-R. 2012 Differences between symmetric and asymmetric facilitation matter: exploring the interplay between modes of positive and negative plant interactions. *J. Ecol.* **100**, 1482–1491. (doi:10.1111/j.1365-2745.2012.02019.x)
- Czaran T, Bartha S. 1992 Spatiotemporal dynamic models of plant populations and communities. *Trends Ecol. Evol.* **72**, 38–42. (doi:10.1016/0169-5347(92)90103-1)
- Farrior CE, Tilman D, Dybzinski R, Reich PB, Levin SA, Pacala SW. 2013 Resource limitation in a competitive context determines complex plant responses to experimental resource additions. *Ecology* **94**, 2505–2517. (doi:10.1890/12-1548.1)
- Thomas SC, Weiner J. 1989 Including competitive asymmetry in measures of local interference in plant populations. *Oecologia* **80**, 349–355. (doi:10.1007/BF00379036)
- Dempster AP, Laird NM, Rubin DB. 1977 Maximum likelihood from incomplete data via the EM algorithm. *J. R. Stat. Soc. B* **39**, 1–38.
- Leisch F. 2004 FlexMix: a general framework for finite mixture models and latent class regression in R. *J. Stat. Softw.* **11**, 1–18. (doi:10.18637/jss.v011.i08)
- Niklas KJ. 1994 *Plant allometry: the scaling of form and process*. Chicago, IL: University of Chicago Press.
- Baddeley A, Turner R. 2005 SPATSTAT: an R package for analyzing spatial point patterns. *J. Stat. Softw.* **12**, 1–42. (doi:10.18637/jss.v012.i06)
- Weiner J, Stoll P, Muller-Landau H, Jasentuliyana A. 2001 The effects of density, spatial pattern, and competitive symmetry on size variation in simulated plant populations. *Am. Nat.* **158**, 438–450. (doi:10.1086/321988)
- Adams TP, Holland EP, Law R, Plank MJ, Raghob M. 2013 On the growth of locally interacting plants: differential equations for the dynamics of spatial moments. *Ecology* **94**, 2732–2743. (doi:10.1890/13-0147.1)
- Berger U, Piou C, Schiffrers K, Grimm V. 2008 Competition among plants: concepts, individual-based modelling approaches, and a proposal for a future research strategy. *Perspect. Plant Ecol. Evol.*



- Syst.* **9**, 121–135. (doi:10.1016/j.jppees.2007.11.002)
39. Rajaniemi TK. 2003 Evidence for size asymmetry of belowground competition. *Basic Appl. Ecol.* **4**, 239–247. (doi:10.1078/1439-1791-00151)
40. Schwinning S, Weiner J. 1998 Mechanisms determining the degree of size asymmetry in competition among plants. *Oecologia* **113**, 447–455. (doi:10.1007/s004420050397)
41. Schiffrers K, Tielbörger K, Tietjen B, Jeltsch F. 2011 Root plasticity buffers competition among plants: theory meets experimental data. *Ecology* **92**, 610–620. (doi:10.1890/10-1086.1)
42. Lin Y, Huth F, Berger U, Grimm V. 2014 The role of belowground competition and plastic biomass allocation in altering plant mass–density relationships. *Oikos* **123**, 248–256. (doi:10.1111/j.1600-0706.2013.00921.x)
43. Stoll P, Weiner J, Muller-Landau H, Müller E, Hara T. 2002 Size symmetry of competition alters biomass–density relationships. *Proc. R. Soc. Lond. B* **269**, 2191–2195. (doi:10.1098/rspb.2002.2137)
44. Hui D, Wang J, Shen W, Le X, Ganter P, Ren H. 2014 Near isometric biomass partitioning in forest ecosystems of China. *PLoS ONE* **9**, e86550. (doi:10.1371/journal.pone.0086550)
45. Niklas KJ, Midgley JJ, Rand RH. 2003 Tree size frequency distributions, plant density, age and community disturbance. *Ecol. Lett.* **6**, 405–411. (doi:10.1046/j.1461-0248.2003.00440.x)
46. Condit R, Sukumar R, Hubbell SP, Foster RB. 1998 Predicting population trends from size distributions: a direct test in a tropical tree community. *Am. Nat.* **152**, 495–509. (doi:10.1086/286186)
47. Eichhorn MP. 2010 Spatial organisation of a bimodal forest stand. *J. For. Res.* **15**, 391–397.
48. Falster DS, Brännström A, Dieckmann U, Westoby M. 2011 Influence of four major plant traits on average height, leaf-area cover, net primary productivity, and biomass density in single-species forests: a theoretical investigation. *J. Ecol.* **99**, 148–164. (doi:10.1111/j.1365-2745.2010.01735.x)
49. Scheffer M, van Nes EH. 2006 Self-organized similarity, the evolutionary emergence of groups of similar species. *Proc. Natl Acad. Sci. USA* **103**, 6230–6235. (doi:10.1073/pnas.0508024103)
50. Wardle JA, Allen RB. 1983 Dieback in New Zealand *Nothofagus* forests. *Pacific Science* **37**, 397–404.